



Contents lists available at ScienceDirect

Materials Today: Proceedings

journal homepage: www.elsevier.com/locate/matpr

Effect of the web, face sides and arc's dimensions on the open top-hat structure performance subjected to a flexural static loading

Samer Fakhri Abdulqadir^a, Alaseel Bassam^{b,*}, M.N.M. Ansari^{b,c}, Rabah S. Shareef^a

^a Department of Mechanical Engineering, University of Anbar, Iraq

^b Mechanical Engineering Department, Universiti Tenaga Nasional (UNITEN), 43000 Kajang, Malaysia

^c Institute of Power Engineering, Universiti Tenaga Nasional (UNITEN), 43000 Kajang, Malaysia

ARTICLE INFO

Article history:

Available online 10 February 2021

Keywords:

Flexural

Top-hat- energy absorption

Maximum force

Bending resistance- quasi-static

ABSTRACT

This paper presents the study of the open-top hat structure subjected to quasi-static loading. The finite element models have been carried out using the nonlinear finite element ABAQUS. The open-top hat structure is mainly used as an energy absorber or as a B-pillar in the side of the car. The B-pillar is usually subjected to a flexural (bending) loading. In this study, the open-top hat structure was used to eliminate the effect of the closure plate on the performance, and to establish the effect of changing the dimensions of the face and web sides on the performance. Despite changing the dimensions of the face and web sides, the perimeter of the open-top hat structure was preserved. The study procedure is divided into three phases. The first phase includes changing the length of the sides of the structure to determine the best dimensions in terms of energy absorption (EA) and the maximum peak force and hence the bending resistance of the structure that represents the higher performance of the structure. The second phase uses different angles between the face side and the web side to determine the effect of angle on the structure performance. The third phase includes changing the top and bottom arc sizes with different values to verify their effect on the structure crashworthiness performance. The results of the first and second phases have shown that the T2 design with a side angle of 94 has an outstanding crashworthiness performance and therefore was the selected to be further enhanced in the third phase. The third phase uses a wide range of the top and bottom arc dimensions to optimise the performance of the structure further. The design R1212 has shown the best performance. It has 14.5% more energy absorption, and 18.8% higher mean load when compared to T2-94.

© 2021 Elsevier Ltd. All rights reserved.

Selection and peer-review under responsibility of the scientific committee of the 3rd International Conference on Materials Engineering & Science.

1. Introduction

Recently, researchers have focused on the thin-walled structures made up of aluminium alloys rather than steel in the vehicle applications because of their lightweights and energy absorption capabilities [1–2]. Among all the geometries used in the car component as energy absorbers, hat-shaped structures are the design that has been widely used in the vehicle structures [3–9]. To investigate the bending mechanism of the top-hat section, for example, k Chang Qi et al. have implemented comparative research on the flexural behaviour of the empty and aluminium foam-filled aluminium-steel hybrid material double hat structure subjected

to lateral loadings. The double-hat structures are proposed as part components used in the vehicles to enhance the crashworthiness performance by increasing the energy absorption and bending resistance. The study has found that incorporated foam filler enhances the specific energy absorption by 30% and the bending moment has doubled compared to empty structure [1]. Libin Duan et al. investigated the theoretical prediction of the thin-walled top hat beam subjected to three-point bending loadings. The study has concluded that the steel-aluminium hybrid structure has absorbed more energy than high-strength steel without exceeding the initial weight [10]. Kentaro Sato et al. carried out quasi-static and dynamic tests on the top hat-shaped made of high strength steel. The structure is used in the side crash tests since the centre of the structure's pillar has the essential roles protecting the occupant's survival distance. The face dimension was 60 mm, the verti-

* Corresponding author.

E-mail address: bsmaq.it@gmail.com (A. Bassam).

cal web dimension was 60mm the top and bottom arc dimension was set as an identical dimension of 5 mm and the angle between the face and web side was 99.5 degree. They concluded that the bending moment increased as the material sheet thickness and material strength increase [11].

Gurpinder S. Dhaliwal and Golam M. Newaz studied a hybrid single hat beam subjected to flexural loadings using three-point bending tests. The section was made of aluminium material adhesively bonded to carbon fibre plies. The purpose of the study was to investigate the utilising of the hybrid composite structure in the automotive industries and compare it to monolithic materials like aluminium and steel. The results have shown that there was a weight saving of 15–25% for the hybrid system compared to the same weight of aluminium [12]. Chang Qi et al. proposed a double top-hat section contained a hybrid aluminum-steel material used in the automotive bumper parts to reduce pedestrian injury. The hybrid structure was set to be of two parts, the top one is the aluminium hat while the bottom one was the steel hat joined by using rivets. The purpose of this arrangement is to reduce the initial force and to increase the specific energy absorption of the structure. The structure was subjected to a lateral loading using a quasi-static three-point bending test. The results have shown that the hybrid structure has better bending resistance compared to the monolithic structure and its recommended for use in the vehicle bumpers [13]. Zhi Xiao et al. investigated a new thin-walled configuration of tailor rolled blank top-hat (TRBTH) which used in the crashworthiness and lightweight applications. The structure was subjected to three-point bending and four point-bending. The characteristic of this configuration is having a thicker wall thickness in the highest load-bearing and thinner thickness in the rest of the regions. It was found that the bending resistance of the (TRBTH) was higher than the uniform thickness at the same mass and the structure is more suitable for use as an energy absorber in car applications [14].

Despite the significant number of works presented on the top-hat structure, no attempts have been made yet to apply the dimension of the top-hat sides, the angle between sides and the effect of arc size on the crashworthiness performance. So, the objective of this study is to find the effect of these parameters on the structure performance to select the structure with the highest performance which means the highest energy absorption capability and highest bending resistance.

2. Material and profile description

The material used in this study is 5754 aluminium alloy. The properties of this material were produced from the tensile test of the standard coupon Fig. 1. The specimens were tested at room temperature with a quasi-static loading of 2 mm/min, the stress-strain data was obtained from the system software and the young modulus of elasticity (E) was calculated from the data obtained. The modulus of elasticity of the material is 68Gpa, Yield stress is 60 MPa, Ultimate tensile stress is 190 MPa, density (ρ) is 2700 kg/m³ and poisson's ratio $\nu = 0.3$.

The current study proposed a structure that consists of an open top-hat profile with two semi-cylinders rigid that mounted under the top-hat to support it. Another rigid cylinder is mounted above the top hat which represents the punch. The punch (the force) is placed in the middle of the structure with a radius of 40 mm and



Fig. 1. Specimen of 5754 alloys used in the study.

a length of 200 mm while the two semi-support cylinders are placed at 25 mm away from each end with a span of 400 mm as shown in Fig. 2.

The top hat length is set to be at a length of 450 mm and the flange width is set as 25 mm. The preliminary length of the face side is set at 43 mm, the web side length is 50 mm, the top arc radii size is 11 mm and the bottom arc radii size is 8 mm. The simulation procedures consist of three phases. The first Phase includes changing the face and the web sides length of the structure to specify the best dimensions in terms of energy absorption (EA) and the maximum peak force and hence the bending resistance of the structure. The second phase is changing the angle between the face side and the web side to determine the effect of angle between sides on crashworthiness performance. In the third phase, after optimising the best structure performance depending on the results obtained in the first and second phases, the change of the radii dimension of both top and bottom arcs is taking place.

In the first phase, the top arc radii are set at 11 mm while the bottom arc radii are set to be 8 mm. The face side is set at 43 mm and the web side is 50 mm so, the perimeter is set to be 143 mm excluding the flanges and the dimension of top and bottom arcs. The simulation processes including change of the face side by increasing the dimension by 5 mm at the same time decreasing the web side by 2.5 mm from each side, so the whole perimeter along this phase will be kept at 143 mm. The face side dimension starts from 43 mm and increases during the first phase until it reaches 83 mm while the web side starts at 50 mm and decreases until it reaches the dimension of 30 mm. The second phase is changing the angle between the face side and the web side. The angles taken in this study are 90, 92, 94, 96, 98 and 100. These angle values are applied synchronising with the change of structure sides in the first phase.

After the best structure is chosen according to the highest performance (higher energy absorption and higher force and hence higher bending resistance), this structure will be further enhanced by using a different top and bottom arc sizes in the third phase. This phase includes using a wide range of arc dimensions starting from 5 mm until 14 mm. The study will be using identical dimension in both the top and bottom arc, enlarges the top arcs and decreases the bottom and vice versa.

3. Finite element models

The non-linear finite element ABAQUS has been used in this study to simulate the structure under quasi-static loads. The structure is an open top-hat beam. The length of the structure has been fixed at 450 mm with a wall thickness of 3 mm. The structure is made of 5754 aluminium series material. The structure is used to imitate the pillars used in the car, especially the B-pillar. The B-pillars in the vehicle usually are subjected to a flexural loading. The structure consists of the top-hat beam with a rigid cylinder with a diameter of 80 mm and a length of 200 mm is placed above the structure that representing the punch hitting the structure. Two semi-rigid cylindrical tubes with a length of 200 mm are mounted beneath the structure to support it during the loading. The thin-walled top-hat beam is modeled as a 4-node (S4R) doubly curved thin shell standard quad, reduced integration, hourglass control and element deletion. The striker cylinder and the two support cylinders are modeled as a 4-node (R3D4) rigid quadrilateral. The mesh size for all the parts in the structure is set to be at 5 mm. The contact between all the parts in the structure is modelled as general contact with a friction coefficient of 0.2 [15–19]. The boundary conditions of the support cylinders are modeled to be fixed in all degrees of freedom while the striker cylinder is mod-

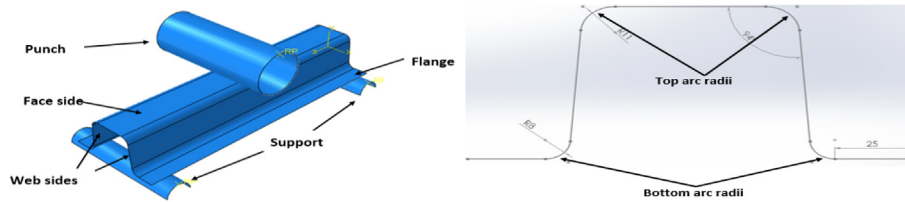


Fig. 2. Design description of the open hat beam.

eled with one translation displacement and it is fixed in other movements.

4. Crash performance indices

The crash performance parameters are very important to select the best structure that has the highest performance which represents the higher energy absorption and higher bending resistance (maximum force). The maximum peak force is generated directly from the software and the highest peak force represents the highest bending resistance which is preferable. The mean force (f_m) is the average force along with the deformed structure and can be calculated by dividing the energy absorbed by the structure to the total deformation length as shown in Eq. (1).

$$f_m = \frac{EA}{d_m} \tag{1}$$

5. Results and discussions

5.1. Changing the face and web sides

In this section, the first phase and the second phase are merged. So, the use of different top-hat sides and the change of the angle between the face and the web sides are discussed. The Name and the dimension of each design are listed in Table 1.

As shown in Table 1, nine different dimensions were used in this study for each angle. The preliminary angle between the face side and the web side was 90 degree. The face side length of the first design (T1) was 43 mm and it was increased by 5 mm for each design until reached the dimension of 83 mm (T9). While the web side of the first design (T1) was 50 mm and it was decreased by 2.5 mm from each side until it reached 30 mm (T9). The flange width from both top-hat sides was also preserved at 25 mm for all different designs. The perimeter of the structure for all designs (T1-T9) was reserved. The purpose of maintaining the same perimeter for all the designs is to specify which design has the highest performance in terms of energy absorption and the bending resistance. The predicted results of all designs for the angle of (90–94) and the angle of (96–100) are listed in Tables 2 and 3, respectively.

Table 1
The definition and dimension of the top-hat design.

no.	Structure name	Face side (mm)	web side (mm)
1	T1	43	50
2	T2	48	47.5
3	T3	53	45
4	T4	58	42.5
5	T5	63	40
6	T6	68	37.5
7	T7	73	35
8	T8	78	32.5
9	T9	83	30

For the side's angle of 90, the maximum force value was 13.6 kN at T1 design while the lowest force value was 10.6 kN at the T9 design when the web side dimension at a minimum value. For the side angle of 92 degree, T1 has the highest force value of 14.1 kN while the T9 has the lowest value of 10.6 kN and the highest energy absorption value was 550 J at the T1 since it has the highest mean load. For the angle of 94, the T1 has the highest peak force value of 14.3 kN while the T9 design has the lowest value of 11 kN. T1, T2, T3 has higher energy absorption (over 500 J) compared to other designs.

The predicted results when the side angles (96–100) are listed in Table 3. For the angle of 96, the highest force value of 14.5 kN was at the T1 design and the lowest value of 11 kN was at the T9 design. The highest energy absorption values (over 500 J) were at the T1, T2 and T3. For the angle of 98, the highest force value of 14.4 was at the T1 design while the T9 has the lowest value of 10.8 kN. The highest energy absorption value was 528 J at the design T2. For the angle of 100, the highest force value of 14.9 was at the T1 design while the T9 has the lowest value of 10.7 kN. The highest energy absorption values were at the T1, T2 and T3 when the Pm at the highest values. For the side's angles of 96, 98 and 100, the maximum force was at T1 design of 14.4 kN, 14.5 kN and 14.9 kN while the minimum force was at T9 of 10.7, 10.8 and 10.9 kN respectively. It can be concluded that the highest force value is when the web side at the maximum value at T1 and the minimum force value was when the web side at the lowest size at T9 and this is due to decrease in the structure stiffness since the web side bears the most load when the structure loaded.

The second phase includes changing the face and web side angle. The predicted results are listed in Tables 2 and 3. The peak force value of the T1 was 13.6 kN when the angle between sides was 90 and it slightly increased with the angle until it reached the highest value of 14.9 kN at the angle value of 100 and the maximum energy absorption was 565 J when the Pm is at its highest value at the side angle of 100. For the T2 design, the peak force was 13.2 kN at the angle of 90 degree and increased slightly until it reached the value of 14.4 at the side angle of 100. The maximum energy absorption was 545 J when the mean force was at the maximum value of 8.5 kN at the side angle of 100. For the T3 design, the peak force at the angle of 90 was 12.9 kN and it almost increased with the angle until it reached 14 kN at the angle of 100. The maximum energy absorption was 524 J at the angle of 96. For the T4 design, there was a minimal gradual increase in the peak force value from 12.8 kN at the angle of 90 until it reached a value of 13.6 at the angle of 100. The maximum energy absorption was 515 J when the mean force at its maximum value of 9 kN at the side angle of 98. For the design T5, the peak force was 12.4 kN at the angle of 90 and it increased with a minimal value with the angle until it reached the maximum value of 13 kN at the side angle of 100. At T5 design, the peak force at the side angle of 90 was 12.4 kN and it increased slightly with the side angle until it reached the highest value of 13 kN at the angle side of 100.

At the T6 design, the peak force at the angle of 90 was 11.9 kN and it increased slightly with the angle until it reached the maxi-

Table 2
Predicted results for the structures with side's angle (90–94).

No.	File name	90			92			94		
		Energy (J)	Peak force (kN)	Mean force (kN)	Energy (J)	Peak force (kN)	Mean force (kN)	Energy (J)	Peak force (kN)	Mean force (kN)
1	T1	439	13.6	7.6	550	14.1	8.8	551	14.3	8.2
2	T2	438	13.2	7	496	13.7	7	532	14	8.0
3	T3	428	12.9	7	505	13.4	7.9	521	13.6	8.4
4	T4	511	12.8	8.5	496	13	7.6	474	13.1	7.5
5	T5	469	12.4	7.4	449	12.5	6.9	487	12.6	7.1
6	T6	457	11.9	7.1	435	12	6.7	450	12.1	6.7
7	T7	463	11.7	7.6	450	12	7.4	436	11.7	7.3
8	T8	475	11	7.3	409	11.1	6.7	485	11.3	8.2
9	T9	417	10.6	7.1	394	10.6	6.7	438	10.8	7.2

Table 3
Predicted results for the structures with side's angle (96–100).

No.	File name	96			98			100		
		Energy (J)	Peak force (kN)	Mean force (kN)	Energy (J)	Peak force (kN)	Mean force (kN)	Energy (J)	Peak force (kN)	Mean force (kN)
1	T1	538	14.4	8.3	474	14.5	8.3	565	14.9	8.6
2	T2	516	14	7.7	528	14.3	8.2	545	14.4	8.5
3	T3	524	13.7	8.4	498	13.8	8.1	518	14	8.4
4	T4	485	13.2	7.6	515	13.4	9.0	499	13.6	8.2
5	T5	471	12.8	7.6	486	13	8.3	482	13	7.9
6	T6	495	12.3	8.3	486	12.4	8.3	482	12.5	7.9
7	T7	450	11.7	7.6	397	11.7	7.4	453	12	7.1
8	T8	469	11.3	8	481	11.4	7.9	460	11.5	8.4
9	T9	403	10.7	6.8	417	10.8	7.1	419	10.9	7

imum value of 12.5 kN at the angle of 100. The maximum energy absorption was 495 J when the mean force was at the highest value of 8.3 kN at the angle side of 96. The peak force of the T7 design at the angle of 90 was 11.7 kN and it reached the maximum value of 12 kN at the side's angle of 100. The maximum energy absorption was 463 J when the mean force was at the highest value. The peak force for the T8 at the side's angle 90 was 11 kN and it slightly increased with the angle until it reached the value of 11.5 kN at the angle value of 100. The maximum energy absorption was 534 J when the mean force at the highest value at the side's angle of 100. The design T9 has a peak force value of 10.6 kN at the angle of 90 and it increased with a very minimal value until it reached a value of 10.9 at the angle of 100. The maximum energy absorption was 438 J when the mean force at the highest value at the side's angle of 94. Figs. 3 and 4 show the maximum force and the energy absorption for each design at the different side angles used in this study.

From the predicted results, it can be concluded that the peak force increases slightly as the side's angle increases and these incremental are at the minimal value because of the slight increase in the web side due to increase in the side's angle. It can also be

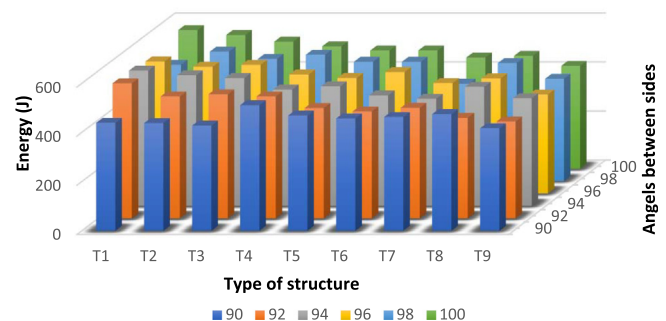


Fig 4. Energy absorption of each design at different side's angles.

concluded that T1, T2 and T3 have almost higher energy absorption. So, among these designs, the T2 design at the side' angle of 94 was chosen and it will be enhanced in terms of changing the top and bottom arc's radii.

5.2. Different arc dimensions

The T2 design with a side's angle of 94 has been chosen to enhance further. The face side is 48 mm and the web side is 47.5 mm. The top arc radii are 11 mm and the bottom arc radii are 8 mm. In this section, the face side, the web side, the flange size and the side's angle will be kept at their values without any change. Both the top and the bottom arc radii will be changed independently. The obtained results will be compared with this design (T2). The design will be named starting with the letter (R) followed by numbers. The first number (numbers) refers to the top arc radii dimension while the other number (numbers) refers to the bottom arc radii dimension. The results are shown in Table 4.

5.2.1. Identical arc size

The simulation process at this stage has begun when the top arc radii and bottom arc radii have the same value. The first arc radii

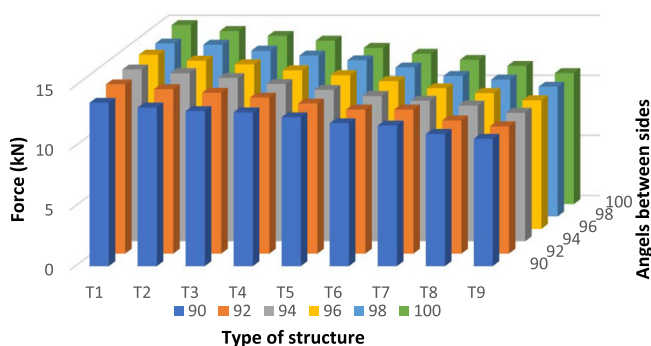


Fig. 3. The maximum force of each design at different side's angles.

Table 4

Predicted results of the structures with different arc dimensions.

	Design-name	Top arc (mm)	Bottom arc (mm)	Energy (J)	Force (kN)	Pm (kN)	Non-dimensional Energy (%)	Non-dimensional force (%)	Non-dimensional mean force (%)
	T2	11	8	532	14	8			
1	R55	5	5	451	11.6	7.8	0.85	0.83	0.98
2	R66	6	6	461	11.9	7.6	0.87	0.85	0.95
3	R77	7	7	502	12.4	8.6	0.94	0.89	1.08
4	R88	8	8	477	13	6.6	0.90	0.93	0.83
5	R99	9	9	486	13.1	7.6	0.91	0.94	0.95
6	R1010	10	10	466	13.3	8.1	0.88	0.95	1.01
7	R1111	11	11	480	13.6	7.6	0.90	0.97	0.95
8	R1212	12	12	609	14	9.5	1.14	1.00	1.19
9	R1313	13	13	566	14.4	8.9	1.06	1.03	1.11
10	R68	6	8	457	12.2	6.9	0.86	0.87	0.86
11	R78	7	8	490	12.6	7.9	0.92	0.90	0.99
12	R98	9	8	508	13.2	8.3	0.95	0.94	1.04
13	R108	10	8	510	13.4	8	0.96	0.96	1.00
14	R128	12	8	451	13.7	7.7	0.85	0.98	0.96
15	R138	13	8	457	13.8	7.8	0.86	0.99	0.98
16	R116	11	6	559	13.7	8.7	1.05	0.98	1.09
17	R117	11	7	537	13.8	8.4	1.01	0.99	1.05
18	R119	11	9	565	13.9	8.9	1.06	0.99	1.11
19	R1110	11	10	541	14.0	8.4	1.02	1.00	1.05
20	R1112	11	12	529	14	7.8	0.99	1	0.98
21	R611	6	11	542	12.6	9.1	1.02	0.90	1.14
22	R711	7	11	495	12.8	7.8	0.93	0.91	0.98
23	R811	8	11	501	13.2	8.4	0.94	0.94	1.05
24	R911	9	11	509	13.5	8.6	0.96	0.96	1.08
25	R1011	10	11	567	13.7	9.2	1.07	0.98	1.15
26	R1211	12	11	555	14.1	9.2	1.04	1.01	1.15
27	R145	14	5	512	13.9	8.2	0.96	0.99	1.03
28	R146	14	6	514	14	7	0.97	1.00	0.88

dimension has been taken at 5 mm for both top and bottom arcs (R55). Through the analysis, the energy absorbed by the R55 design was 451 J, the peak force was 11.6 kN and the mean force (Pm) was 7.8 kN. when compared these results to T2, this R55 has lower performance than T2 since it has 15% lower absorbed energy, 17% lower peak force and 2% lower Pm. For the arc radii of 6 mm (R66), this structure has 13% lower energy absorption, 15% lower peak force and 5% lower Pm. The R77 (top and bottom arcs radii of 7 mm) the structure has a higher performance than R55 and R66. The R77 design has absorbed 6% less than T2, 11% lower in peak force while the Pm was enhanced by 8%. The R88 design has 10% lower energy absorption, 7% lower in peak force and 17% lower in Pm compared to the T2. For the R99, the predicted results have shown the design has 9% lower in energy absorption, 6% lower in peak force and 5% lower in Pm when compared with T2. The R1010 has 12% less energy absorption, 5% less peak force while the Pm was enhanced by 1%. The results of the R1111 design have shown that it has 10% lower energy absorption, 3% lower in Peak force and 5% lower in Pm compared to T2. The R1212 design has 14% higher energy absorption and 19% higher Pm when compared with the T2. So, this design has better crashworthiness performance than T2. The R1313 design has 6% more energy absorption, 3% higher peak force and 11% higher Pm than T2. From the previous result of using identical size for both top and bottom arcs, it can be concluded that the peak force increases as the arc size increases and the higher energy absorption are when the mean force at the higher value. The best design was when the top and bottom arc radii dimension of 12 mm at the face side is 48 mm and the web side is 47.5 mm

5.2.2. Non-Identical arc size

5.2.2.1. Changing the top arc radii dimension with maintaining the bottom arc at 8 mm.

This section is taking inconsideration the results of the designs that have different arc's size. The design R68 (top arc radii of 6 mm and bottom arc radii of 8 mm). This

design has a lower performance than T2 since it has 14% lower energy absorption, 13% lower peak force and 14% lower Pm. The R78 design has 8% lower energy absorption, 10% lower peak force and 1% lower in Pm when compared with the T2. The results of the R98 structure has revealed a decreasing in energy absorption by 5%, decrease in the peak force by 6% while showed an enhancement in the Pm by 4% compared with the T2. The R108 (top arc of 10 mm and a bottom arc of 8 mm) has 4% lower in energy absorption, 4% lower peak force while the Pm has the same value when compared with the T2. The R128 structure has a lower performance than T2 since it revealed lower absorbed energy by 15%, lower peak force by 2% and lower Pm by 4%. For the R138 structure, it has a lower performance than T2 since it showed lower energy absorption by 14%, lower peak force by 1% and lower Pm by 2%. The previous results have taken in consideration that the structure has a bottom arc radius of 8 mm as in the T2, while the top arc radii have been taken in the range of 5–13 mm (smaller and larger than) T2 (11 mm). The results have emphasised that the peak force increases as the top arc radii increase [table 4](#).

5.2.2.2. Changing the bottom arc radii dimension with maintaining the top at 11 mm.

In this section, the analysis was done by using the top structure arc radii of 11 mm as same as in T2 with taking the bottom arc radii dimension with different values (smaller and larger than 8 mm). The R116 design has a top arc radius of 11 mm with a bottom arc radius of 6 mm. Compared to T2, the R116 has 5% more absorbed energy, 2% lower in Peak force and 9% higher in Pm. The R117 structure has a top arc radius of 11 mm with a bottom arc radius of 7 mm. This design has 1% more energy than T2, 1% lower in peak force and 5% more in Pm. The R119 has an increase in energy absorption by 6%, lower in peak force of 1% and enhancing in the Pm by 11% compared to T2. For the R1110, the structure has a top arc radius of 11 mm with a bottom arc radius of 10 mm. Compared to the T2 design, the R1110 has 2% more energy absorption, the same peak force and an increase in

the Pm by 5%. The predicted results of the R1112 design have 1% less energy absorption and 2% less in the mean force while the peak force was at the same value. From the obtained results, it can be concluded that when the top arc radius is fixed 11 mm as in T2, the peak force of the structure increases as the bottom arc radius increase and the mean force and energy absorption have enhanced in all arc size values since the top arc dimension is larger than the bottom one.

5.2.2.3. Changing both the top and the bottom arc radii dimensions. In this section, the different top and bottom arc's size values have been used. The R611 design has a top arc radius of 6 mm and a bottom one of 11 mm. Compared to T2 design, the R611 has absorbed 2% more energy with a 10% lower peak force and has 10% higher in mean force. The R711 design has 7% lower energy, 9% lower in peak force and 2% lower in the mean force compared to T2. The R811 design has 6% less energy absorption, 6% less peak force and the mean force has improved by 5%. compared with the T2. The R911 has 4% lower energy absorption, 4% lower peak force with an increase in mean force by 8%. compared with the T2. The results are tabled in Table 4.

The R1011 (top arc radius is 10 mm and the bottom is 11 mm), has 7% more energy absorption, 2% lower in peak force and the mean force has improved by 15%. Compared with the T2. The results of the R1211 has 4% lower energy absorption, 1% lower in peak force and 3% higher in mean force compared to T2. The predicted results of the R146 design has 3% lower in energy absorption and 12% lower in the mean force compared to T2. The results are tabled in Table 4. When comparing a structure that has a large top arc size and low bottom arc size with a structure that has a low top arc size and large bottom arc size, the structures with large top arc reveal higher crashworthiness performance than a structure has a low top arc for the equivalent arc dimensions Fig. 5. Since the failure of the structure and the stress concentration will be found at the top arc as shown in Fig. 6.

6. Conclusion

The B-pillar structure is used as an energy absorber in the side of the car. It is usually subjected to a flexural (bending) loading. The study has used an open-top hat structure subjected to quasi-static loading because the effect of changing in side dimensions and angles will be obvious and the study has ignored the closure plate aiming to specify which side of the structure has more influence on its performance. The perimeter of the open-top hat structure was preserved. The study procedure was divided into three stages. The first stage included changing the dimensions of the sides of the structure to specify the best dimensions in terms of energy absorption (EA) and the maximum peak force and hence the bending resistance of the structure. The second stage included changing the angles between the face side and the web side to

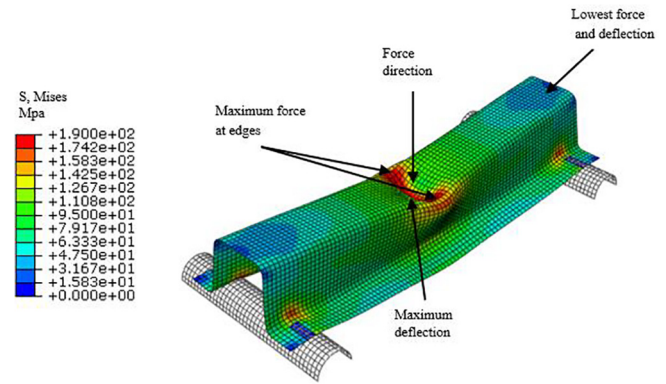


Fig. 6. Finite element model of the top hat beam.

determine the effect of the angle on the structure performance. From the first and second phase, the higher structure performance was chosen. The third stage included changing the top and the bottom arc sizes of the selected structure with different values to determine their effect on the structure crashworthiness performance. Despite the significant number of works presented on the top-hat structure, no attempts have been made yet to apply the dimension of the top-hat sides, the angle between sides and the effect of arc size to improve the crashworthiness performance. So, the study aimed to find the effect of these parameters on the structure performance. The study has concluded the following:

- The maximum peak force increases as the web side increases (face side decreases) this is due to the increases in the structure stiffness since the web side bear the most load when the structure loaded. So, the highest force value is when the web side at its maximum value
- The peak force slightly increases as the side's angle increases. This minimal increase is contributed mainly to the slight minute increase in the length of the web side.
- The T2-94 design was chosen after stage one and two to be a reference design for the third stage due to higher energy absorption and bending resistance. This has a side angle of 94, face side of 48 mm and web side of 47.5 mm.
- When comparing a structure that has a large top arc and small bottom arc (Tb) with a structure that has a small top arc and large bottom arc (tB), the large top arc structure reveals higher crashworthiness performance than a structure has a large bottom arc for the equivalent arc dimensions Fig. 5. So, the performance of the R116, R117, R118, R119, and R1211 is higher than (R611, R711, R811, R911, and R1112). This is because the failure of the structure and the stress concentration will be found at the top arc as shown in Fig. 6.
- The peak force and the mean force of the structure with different arc dimension are larger than the structure that has an identical top and bottom arc dimension for the equivalent sizes. This leads to the conclusion that the performance of R117, R146 and R119 is higher than R99 and R1010.
- In general, increasing the top or the bottom arc dimension leads to an increase in the peak force load of the structure.
- The structure that has an identical top and bottom size of 12 mm (R1212) with a face side of 48 mm, web side of 47.5 mm was the best choice since it has 14.5% more energy absorption and 19% higher in mean load when compared to T2-94 with the original arc dimension R118 so, the bigger arc dimension, the better crashworthiness performance since the arcs bear the most load and hence the highest peak force.

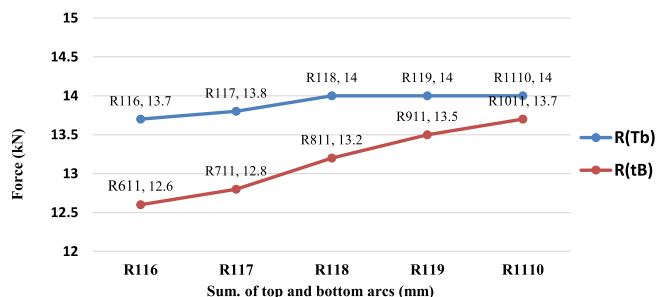


Fig. 5. Peak force vs equivalent arc radius dimensions of the corresponding structures.

CRedit authorship contribution statement

Samer Fakhri Abdulqadir: Conceptualization, Methodology, Software, Writing - original draft. **Alaseel Bassam:** Data curation, Validation, Writing - review & editing. **M.N.M. Ansari:** Visualization, Supervision, Writing - review & editing. **Rabah S. Shareef:** Validation, Methodology.

Declaration of Competing Interest

The authors declare that they have no known competing financial interests or personal relationships that could have appeared to influence the work reported in this paper.

References

- [1] C. Qi, Y. Sun, S. Yang, A comparative study on empty and foam-filled hybrid material double-hat beams under lateral impact, *Thin-Walled Struct* 129 (2018) 327–341.
- [2] S. Chahardoli, A.A. Nia, Investigation of mechanical behavior of energy absorbers in expansion and folding modes under axial quasi-static loading in both experimental and numerical methods, *Thin-Walled Struct* 120 (2017) 319–332.
- [3] G. Sun, M. Deng, G. Zheng, Q. Li, Design for cost performance of crashworthy structures made of high strength steel, *Thin-Walled Struct* 138 (2019) 458–472.
- [4] G. Sun, H. Zhang, G. Lu, J. Guo, J. Cui, Q. Li, An experimental and numerical study on quasi-static and dynamic crashing behaviors for tailor rolled blank (TRB) structures, *Mater. Des.* 118 (2017) 175–197.
- [5] R. Subbaramaiah, B.G. Prusty, G.M.K. Pearce, S.H. Lim, R.S. Thomson, Crashworthy response of fibre metal laminate top hat structures, *Compos. Struct.* 160 (2017) 773–781.
- [6] Z. Xiao, F. Mo, D. Zeng, C. Yang, Experimental and numerical study of hat shaped CFRP structures under quasi-static axial crushing, *Compos. Struct.* 249 (May) (2020) 112465.
- [7] Q. Liu, Z. Ou, Z. Mo, Q. Li, D. Qu, Experimental investigation into dynamic axial impact responses of double hat shaped CFRP tubes, *Compos. B Eng.* 79 (2015) 494–504.
- [8] T. Matsuo, M. Kan, K. Furukawa, T. Sumiyama, H. Enomoto, K. Sakaguchi, Numerical modeling and analysis for axial compressive crushing of randomly oriented thermoplastic composite tubes based on the out-of-plane damage mechanism, *Compos. Struct.* 181 (2017) 368–378.
- [9] Q. Liu, H. Xing, Y. Ju, Z. Ou, Q. Li, Quasi-static axial crushing and transverse bending of double hat shaped CFRP tubes, *Compos. Struct.* 117 (2014) 1–11.
- [10] L. Duan, Z. Du, H. Jiang, W. Xu, Z. Li, Theoretical prediction and crashworthiness optimisation of top-hat thin-walled structures under transverse loading, *Thin-Walled Struct.* 144 (April) (2019) 106261.
- [11] K. Sato, T. Inazumi, A. Yoshitake, S.-D. Liu, Effect of material properties of advanced high strength steels on bending crash performance of hat-shaped structure, *Int. J. Impact Eng.* 54 (2013) 1–10.
- [12] G.S. Dhaliwal, G.M. Newaz, Experimental and numerical investigation of flexural behavior of hat sectioned aluminum/carbon fiber reinforced mixed material composite beam, *Compos. Part B Eng.* 182 (November 2019) (2020) 107642.
- [13] C. Qi, Y. Sun, H.-T. Hu, D.-Z. Wang, G.-J. Cao, S. Yang, On design of hybrid material double-hat thin-walled beams under lateral impact, *Int. J. Mech. Sci.* 118 (2016) 21–35.
- [14] H. Zhang, G. Sun, Z. Xiao, G. Li, Q. Li, Bending characteristics of top-hat structures through tailor rolled blank (TRB) process, *Thin-Walled Struct.* 123 (2018) 420–440.
- [15] Improved vehicle crashworthiness design by control of the energy absorption for different collision situations, 1999.
- [16] S.F. Abdulqadir, Design a new energy absorber longitudinal member and compare with S-shaped design to enhance the energy absorption capability, *Alexand. Eng. J.* 57 (4) (Dec. 2018) 3405–3418.
- [17] Z. Ahmad, D.P. Thambiratnam, Dynamic computer simulation and energy absorption of foam-filled conical tubes under axial impact loading, *Comput. Struct.* 87 (3–4) (2009) 186–197.
- [18] B. Dehghan-Manshadi, H. Mahmudi, A. Abedian, R. Mahmudi, A novel method for materials selection in mechanical design: combination of non-linear normalisation and a modified digital logic method, *Mater. Des.* 28 (1) (2007) 8–15.
- [19] F. Tarlochan, F. Samer, A.M.S. Hamouda, S. Ramesh, K. Khalid, Design of thin wall structures for energy absorption applications: enhancement of crashworthiness due to axial and oblique impact forces, *Thin-Walled Struct.* 71 (2013) 7–17.